

# Endogenous neurogenesis, histological and behavioral monitoring of recovery of paraplegia, after total spinal cord transection in mice

## Abstract

Mice, in contrast to other species, have the ability to recover after severe spinal cord damage without any therapeutic intervention. We studied the development of Wallerian degeneration of the long spinal tracts and also the contribution of proliferative neuronal and glial cells after complete spinal cord transaction including the dura mater in C57bl/6 mice. In addition, we monitored the functional recovery in association with histological and immunohistochemical observations. Critical point of time after SCT was the second week, when the lesion reached its maximum size, was well-vascularized and begun to self-limit drastically, thereafter. However, slight degree of functional recovery began from 48 hours after spinal cord transection. Immunophenotype analysis of the proliferative cells revealed that endogenous neurogenesis was of the glial, and not of the neuronal cell-type proliferation. Glial cells seemed to almost completely replace cellular loss, to remyelinate spared axons, to restore blood barrier and to support the rest, undamaged, neurons. Intense proliferation of glial cells occurred in the first 48 hours after injury and began to decline thereafter. Consequently, therapeutic interventions aiming at stimulation of endogenous neurogenesis should be initiated within the first hours after injury, while new approaches should target at stimulating not only the glial but also the endogenous neuronal cell-type proliferation.

**Keywords:** Endogenous neurogenesis, Spinal cord transaction

Volume 6 Issue 1 - 2016

Evangelia Athanasiou,<sup>1</sup> Damianos Sotiropoulos,<sup>1</sup> Eleni Siotou,<sup>1</sup> Konstantinos Violaris,<sup>2</sup> Mattheos Bobos,<sup>3</sup> Athanasios Fassas,<sup>1</sup> Achilles Anagnostopoulos<sup>1</sup>

<sup>1</sup>Department of Haematology and Bone Marrow Transplantation, George Papanicolaou Hospital, Greece

<sup>2</sup>Department of Neurosurgery, George Papanicolaou Hospital, Greece

<sup>3</sup>Department of Pathology, Aristotle University Medical School, Greece

**Correspondence:** Evangelia Athanasiou, Department of Haematology and Bone Marrow Transplantation, George Papanicolaou Hospital, 17th Noemvri 9 street, 55534, Pylaia, Thessaloniki, Greece, Tel 30 6977 646687, Fax 30 2310 236279, Email evathanasiou@hotmail.com

**Received:** October 14, 2016 | **Published:** October 14, 2016

## Introduction

Severe spinal cord injury usually leads to permanent loss of locomotor function in rodents and even more in humans.<sup>1,2</sup> Partial sparing of function has been reported in mice which, in contrast to rats, exhibit substantial improvement over time. Rather surprisingly, the histopathological responses to various spinal cord injuries (weight-drop, ischemic, hemi-section, and transection) are quite different in mice than rats.<sup>3-6</sup> For experimental purposes, non-aggressive injury models have been used in most studies, because they are similar to spinal cord damage in humans. In addition, rats are preferable to mice, because spinal cord injury in rats undergoes almost the same clinical and histological process as in humans over time. In contrast, mice have the ability to overcome even severe spinal cord damage, while rats and humans have a slow and very limited recovery. It is still unknown why superior mammals have “lost”, probably during their evolutionary differentiation, the ability to reconstitute their tissue damage, and it is also unknown whether we could “wake up” remodelling procedures.

Few studies have investigated the histological and genetic differences in cellular response to injury between species.<sup>3,5,7,8</sup> In the present study, we designed and performed an aggressive experimental model of complete spinal cord transection (SCT) in C57bl/6 mice. The choice of mice was made because these rodents appear to have a self-recovery mechanism, as mentioned above. Clinical tests were performed and were correlated with the morphologic evidence of Wallerian degeneration and wound healing process of the spinal cord. We focused on the investigation of the nature, distribution, and fate of the proliferative cells in the white and gray matter from day 2 to the 3<sup>rd</sup> week after SCT.

## Material and methods

### Animals

A total of 48 adult female C57bl/6 mice (10-12 weeks of age; 20-22gr weight) were sacrificed at 48 hours and at one, two, three, five, eight, nine, ten and eleven weeks after spinal cord injury, and the vertebral columns were histologically and immunohistochemically evaluated. Mice were functionally assessed before biopsies. Six animals died during the post-operative period: two immediately after transection, two after 48 hours, and two after one week. Two animal spinal cords were rammed by osseous emboli from the vertebrae during the surgical procedure and were excluded from the study. All animals were housed and manipulated according to the European Directive (EEC/ 609/86) on Experimental Animal Protection.

### Spinal cord transection

All mice underwent spinal cord transection in an open operation. En hydrous chloral was used for general anesthesia. The injury was performed with a micro (No.11) scalpel and resulted in a complete transection including the dura mater and the whole circumference of the cord at the T10-T11 inter-vertebral space. Povidone iodine was applied for disinfection before and after operation. Animals were kept under low pathogen conditions and received no antibiotics or any other medication.

### Functional assessments

Functional deficits and recovery over time were evaluated by testing the hind limb reflex and coordinated motor function<sup>9</sup> applying 4 motor and 3 sensor tests. Motor tests included: motor score (0-6), platform hung (0-3), wire mesh descent (0-4), and rope walk (0-4). Sensor tests

included: toe spread (0-3), pain withdrawal (0-3) and hind foot bar grab (0-3). The scoring of functional assessment was correlated with histopathological outcomes of recovery and immunohistochemical findings. The day before surgery, mice were behaviorally tested in order to assess their basic performance and were retested on day 2 and at 1, 3, 5, 8, 9, 10, and 11 weeks postoperatively. Both hind limbs were examined in each animal. All tests were independently evaluated by two observers.

### Tissue preparation

Mice were lethally anesthetized and a segment of vertebral column including the lesion region was dissected. The lesion point was labeled with surgical catgut on the skin after transection. The dissected segment consisted of 5 cranial and 5 caudal vertebrae of the lesion point. The specimens were consolidated on pieces of cork with plastic needles in order to avoid more convexion of vertebrae during decalcification with the Mielodex reagents system (5 hours in reagent A and 18-24 hours in reagent B; Bio-Optica, Milan, Italy). Subsequently, the specimens were rinsed in running water and were processed for standard paraffin embedding. Longitudinal samples of 3 $\mu$ m were cut as serial sections for histological and immunohistochemical analysis. Standard procedures were used to generate hematoxylin/eosin (H/E) counter stain, Van Gieson and Luxol Fast Blue histostains.

### Measurement of spinal cord injury

The spinal cord lesion in the mice was asymmetric and did not form a simple cone shape cranially and caudally from the epicenter, as occurs in rats and other mammals. More asymmetric and irregular was the form of restoration of gray and white matter. For these reasons, the extent of the injury was estimated in longitudinal median sagittal sections including the lateral funiculus of white matter, lateral horn of gray matter and central canal. Also, cross sections were also taken as serial sections (Figure 1a&b). The extent of the white and gray matter lesions was measured from the cranial to the caudal boundaries of cyst formation, neural cell damage and white matter demyelination, in Luxol Fast Blue and H/E stains. The lesion was measured in mm<sup>2</sup> contralaterally to the epicenter in the white and gray matter. The extension of scar formation was calculated in two dimensions in Van Gieson stain (Figure 1c). The vertical length of the scar was measured in the widest area of the lesion. The percentage of the length of horizontal scar formation was estimated according to following:

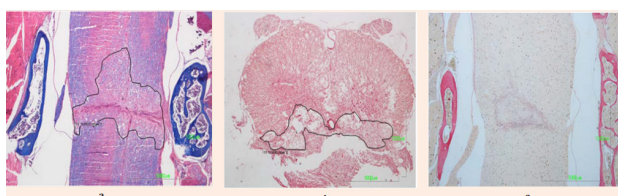


**Figure 1a&1b** The extent of the spinal cord injury was estimated in midsagittal sections in Luxol Fast Blue stain and serial cross sections.

**Figure 1c** The percent of fibrotic displacement of the spinal cord was estimated according to the following type in Van Gieson histostain.

Measurements were performed using the Nikon DS-Qi 1M image analysis system with DS camera control unit DS-L2.

Results are expressed as the average  $\pm$  SD from all animals analyzed. Groups were assessed with regard to different time of sacrifice (2, 7, 21, 35, 56, 63, 70 and 77 days). Differences between groups were determined by the Student's t-test. Values of  $p < 0.05$  were considered statistically significant.

### Immunohistochemistry

In order to detect the type of cells participating in spinal cord restoration, a panel of antibodies was applied for immunohistochemical analysis in 3 $\mu$ m sections. These were antibodies binding synaptophysin (Neo Markers, Fremont CA, 1:100, RB-1461), neurofilament (Neo markers, 1:50, clone 2F11), glial fibrillary acidic protein (Neo Markers rabbit polyclonal anti-GFAP, 1:200), S-100 protein (Neo Markers, 1:100, clone 4C4.9), CD34 (Neo Markers, 1:200, clone Q Bend/10), epithelial membrane antigen (Neo Markers, 1:50.), and CD68 (Neo Markers, 1:40, clone KP1). Heat induced epitope retrieval with citric acid buffer pH 6.0 took place in a microwave oven for 14 min for S-100 protein and CD68, and was followed by overnight incubation with primary antibodies. Visualization was performed using the EnVision System (DakoCytomation).

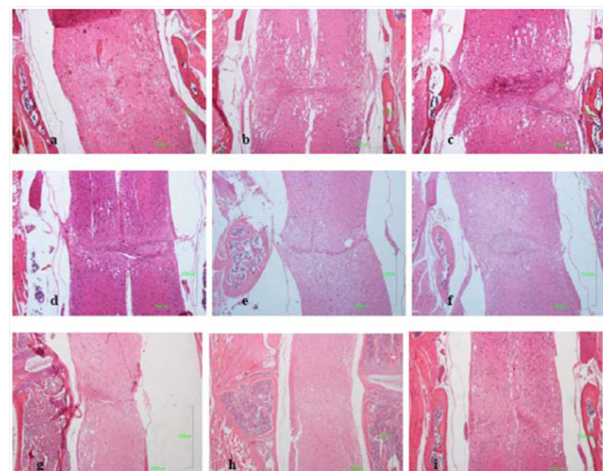


**Figure 2** Longitudinal mid-sagittal E/H sections:

- a. Forty eight hours after SCT the injured area was edematous with hemorrhagic and inflammatory infiltration and debris. Clusters of mineralized axons and axonal spheroids were present mostly in white matter. Micro cyst formation of glia appeared in both sides of the lesion.
- b. One week after SCT the injured area was very extensive with newborn vessels and numerous macrophages phagocytizing debris. Micro cystic cavitation was evident especially in white matter. Central chromatolysis of neural cell bodies and "red" neurons were found in gray matter.
- c. Two weeks after SCT the Periosteal connective tissue from the adjacent vertebrae and from the dura mater separated the spinal cord in two parts, dorsal and caudal. Micro glial nodules appeared at both sides of the lesion.
- d. Three weeks after SCT the micro glial nodules consisted of oligodendrocytes; foamy macrophages penetrated the collagenous trabeculae. Cavitation consisting of small cysts was filled by tissue elements.
- e. Five weeks after SCT the initial lesion began to self-limit. Connective tissue fibers were ill-defined and appeared separated in white matter.
- f. Eight and nine weeks after SCT the micro glial nodules were evident especially in gray matter. The restoration began from the white matter of lateral funiculus. Large numbers of red neurons in clusters were present in distant sites from the initial lesion.
- g. Ten and eleven weeks after SCT the connective tissue continued to regress and was limited in gray matter. The larger part of the lateral funiculus was almost reconnected.

### Double immunostaining for Ki-67 with synaptophysin, GFAP and S-100 protein

In order to avoid the limited reaction of the proliferation marker

Ki-67 (DakoCytomation, Glostrup Denmark) in decalcified tissues, we obtained spinal cord specimens after intra cardiac perfusion with 4% paraformaldehyde in 0.1M phosphate buffer, pH 7.4. The vertebral columns were removed and the spinal cord was pulled out of the vertebral canal. The material was post fixed by immersion in paraformaldehyde buffer 4% for 4-6 hours and was processed for standard paraffin embedding. Serial sections of 3 $\mu$ m were obtained. Before incubation with primary antibody, sections were placed in citrate buffer pH 6.0 and were heated in a microwave oven for 20 min. in 750W. The next step was overnight incubation of sections with anti-Ki-67 primary antibody (1:20) and visualization with the En Vision system. After the development of chromogen (3,3' Diaminobenzidine-DAB), a second incubation of sections with synaptophysin, GFAP, and S-100 antibodies followed. The secondary antibody was biotinylated polyvalent immune globulins. Then, sections were incubated with streptavidin/horseradish peroxidase. The second chromogen was 3-amino-9-ethylcarbazole-AEC. The number of double stained cells was counted in a distance of two vertebrae contralaterally to the epicenter, which included the initial lesion and the whole degeneration area of the white and gray matter.

## Results

### Histopathological and immunohistochemical observation of spinal cord restoration

**Forty eight hours until two weeks after SCT:** Forty eight hours after transection the injured area (average extent 1,75mm<sup>2</sup>  $\pm$  STDEV 0,11) was edematous with hemorrhagic infiltration, loss of all types of neural cells and debris. Clusters of mineralized axons had a superficial resemblance to fungal hyphae and axonal spheroids were present mostly in the white matter (Figure 2). The dura matter was cut and inflammatory cells (neutrophils and macrophages) infiltrated the injured site (Figure 2a). “Red neurons” were not present. Until the second week the lesion grew extensive and reached its maximum size (average extent 2,38 mm<sup>2</sup>  $\pm$  STDEV 0,34). Periosteal connective tissue from the adjacent vertebrae and from the dura matter contributed to fibrotic scar formation which separated entirely the spinal cord in two parts, cranial and caudal (Figure 2b) In the white matter, degenerative changes were apparent, especially in the dorsal column, where damaged nerve fibers of the long ascending and descending tracts underwent Wallerian degeneration (Figure 2c). “Sattelitosis” of oligodendrocytes around neurons and hypertrophic bi nucleated astrocytes were found in the adjacent areas of the lesion epicenter. They formed a dense fibrillary gliosis without penetrating the scar (Figure 3 GFAP). Microcystic cavitation was evident, especially in the white matter. Central chromatolysis of neural cell bodies and “red” neurons were found in the gray matter mostly cranially to the epicenter. The dura matter “invaded” the lesion participating in the fibrotic formation.

**Three and five weeks after SCT:** After the second week the lesion began to regress dramatically (average extent 1,38 mm<sup>2</sup>  $\pm$  STDEV 0,22) (the difference between the extent of the lesion of second and third week was statistical significant  $p \leq 0,05$ ) but the fibrotic scar remained in the same side. Astrocytes began to form a network inside the lesion (Figure 3). Neuronal axons were visible in the scar and neuronal fibers of radices invaded the fibrotic tissue trying to “bridge” the lesion. Neural cell bodies were not present inside the connective tissue (Figure 3). Micro glial nodules were present consisting of oligodendrocytes and foamy macrophages surrounded by collagenous trabeculae. The small cysts of cavitation were now filled with tissue elements (Figure 2d). At fifth week the connective tissue fibers were thinner and appeared separated in selected locations in the white matter

(Figure 4). In these areas, oligodendrocytes and astrocytes formed, between the fibers, a supportive network capable of neuronal axon conjugation (Figure 3). The neuronal axons of radices participated in the restoration, “bridging” the cranial and caudal axons of the white matter (Figure 3 NF). Micro glial nodules were confined inside the gray matter (Figure 2e).

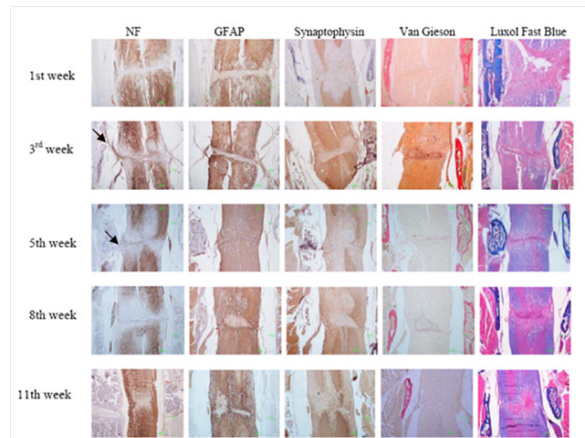


**Figure 3** Immunohistochemical description of neuronal axons (anti-NF), astrocytes (anti-GFAP) and neurons (anti-synaptophysin) during eleven weeks post injury. The lesion site was irregularly shaped, populated by micro glial nodules after the 3<sup>rd</sup> week. Neuronal fibers of radices invaded the fibrotic tissue trying to bridge the lesion in the 3<sup>rd</sup> and 5<sup>th</sup> weeks (arrows). The reconnection of white mater axons began in the 8<sup>th</sup> week and was almost complete in the 11<sup>th</sup> week. Astrocytes (anti-GFAP) began to invade the scar in the 5<sup>th</sup> week forming an astrocytic network, but they remained around micro glial nodules. Neurons (anti-synaptophysin) never invaded the scar but approached the ends of the lesion in the 11<sup>th</sup> week. In the 1<sup>st</sup> week the fibrotic scar (Van Gieson) was already formed with an ill-defined network of connective tissue. Periosteal connective tissue from the adjacent vertebrae and from the dura matter contributed to the fibrotic scar formation which separated the spinal cord in two parts (3<sup>rd</sup> week) and regressed significantly after the 5<sup>th</sup> week. Also, the remyelination of the white mater (Luxol Fast Blue) was remarkable after the 5<sup>th</sup> week.

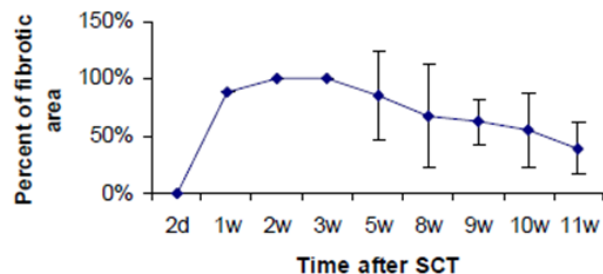


**Figure 4** The fibrotic tissue appeared in the 1<sup>st</sup> week and was completely formed in the 2<sup>nd</sup> and 3<sup>rd</sup> weeks. It covered the entire width of the epicenter, dividing the spinal cord in two entirely separated parts. After the 3<sup>rd</sup> week it began to withdraw and was almost obliterated in 11<sup>th</sup> week.

**Eight to eleven weeks after SCT:** The lesion regressed considerably after eight weeks (average extent 0,69-0,67 mm<sup>2</sup>  $\pm$  STDEV 0,06) and the connective tissue was finally confined inside the gray matter (Figure 3 & Figure 4) The fibers were ill-defined and separated. Micro glial nodules were evident in both the white and gray matter. They extended to a long distance from the initial lesion site and penetrated the fibrotic tissue (Figure 2 f, g). Inside the astrocytic network, undamaged neuronal axons reached both sites of the scar and penetrated the fibrous tissue reconnecting the white matter. In the gray matter neuronal cells approached the ends of the lesion (Figure 3) but

there was no apparent reconnection. Large numbers of “red neurons” in clusters were present in distant sites from the initial lesion.

**Red neurons:** The number of “red neurons” was counted in E/H stain in a distance of 5mm contralaterally to the lesion. “Red neurons” were recognized by their shrunken cell body and intense cytoplasmic eosinophilia with complete loss of Nissl basophilia. Their nucleus was dark and usually lacked the distinguishable nucleolus (Figure 5). Two days after spinal cord damage no “red” neurons were present. They only began to appear in clusters away from the lesion site one week after SCT and their highest number was observed during the 9<sup>th</sup> week (Figure 5).

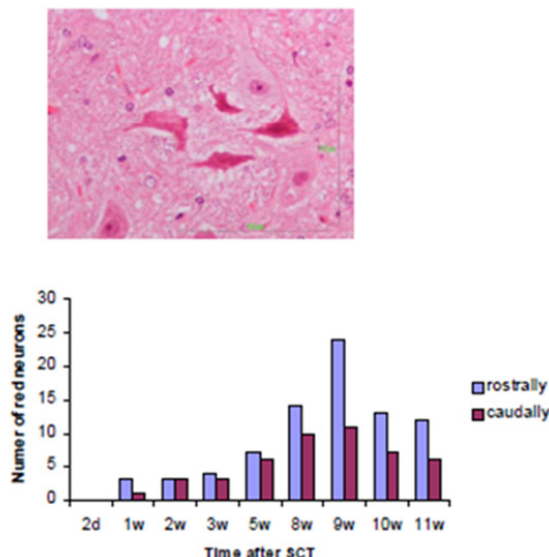


**Figure 5** “Red neurons” were the result of pre-lethal injury of neuronal bodies. They were recognized from their shrunken cell body and intense cytoplasmic eosinophilia with complete loss of Nissl basophilia. Their nucleus was dark and usually lacked the distinguishable nucleolus. They were found in large numbers in the cranial site 9 weeks after injury, although the reconstitution of the injured spinal cord was almost complete.

**Ki-67 analysis:** Double immune stains for GFAP, S-100, synaptophysin, and rat anti-mouse Ki-67 were performed to detect the proliferative status of neurons and their supportive cellular population until 3 weeks after SCT. No neuron bodies were found positive for Ki-67 and synaptophysin double stain. In contrast, the highest number of proliferative astrocytes (Ki-67+/GFAP+) (Figure 6) was found on day 2 after SCT in the cranial part of the lesion ( $204 \pm \text{STDEV } 3,6$ ) (Figure 6a). Their number declined significantly three weeks after SCT ( $49 \pm \text{STDEV } 2,18$ ) (Figure 6d). Proliferative astrocytes showed peri-neuronal “satellitosis” supporting the remaining neuron cells (Fig. 5b) and creating the reactive astrogliosis as a response to injury. In addition, proliferative glial cells (Ki-67+/S-100+) appeared in large numbers on day 2 after SCT also in the cranial part of the lesion ( $200 \pm \text{STDEV } 2,34$ ) (Figure 7a & b). Their number declined after three weeks ( $36 \pm \text{STDEV } 2,16$ ) (Figure 7c), but we observed scattered proliferative cells in micro glial nodules until 5 weeks after spinal cord damage (data not shown). Positive cells for the Ki-67 marker were found, especially in samples of two days after SCT, covering the central canal and corresponding to ependymal cells. Small cells with morphology of micro glial cells with hardly distinguishable cytoplasm and a small dark nucleus were found in the gray matter. In the undamaged spinal cord of a non transected mouse which was used as control, no proliferative glial cells or neuronal bodies were found, except for scattered proliferative micro glial cells.

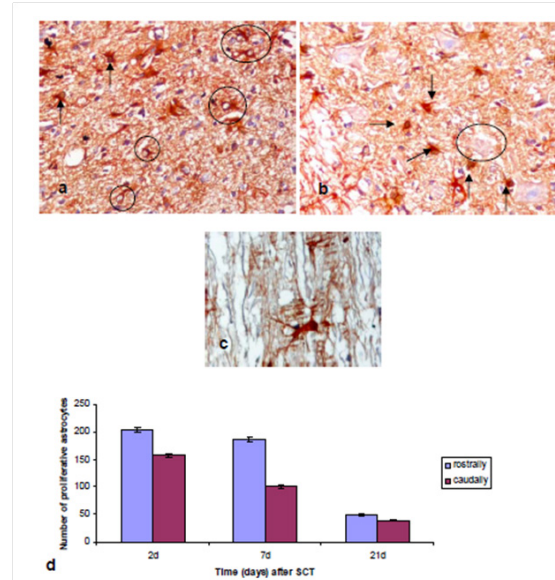


**Figure 6**

- Proliferative astrocytes had red cytoplasm (GFAP) and dark brown nucleus (Ki-67) (arrows). Non-proliferative astrocytes expressed only red cytoplasm and hematoxylin nucleus (encircled cells).
- Proliferative astrocytes (arrows) were arranged around neurons (encircled cell) -perineuronal satellitosis- supporting the remaining neurons and creating reactive astrogliosis which may be a response to injury.
- Proliferative astrocyte in white mater.
- The highest number of proliferative astrocytes was found 2 days after SCT, especially in the cranial site, where the lesion of dorsal tracts was larger; their number declined after the 1<sup>st</sup> week.

**Revascularization of the initial lesion site:** In order to investigate the vascularization of the lesion and the fibrotic scar we performed anti-CD34 immunostain for endothelial cells. Two days after transection there were no well-formed vessels in the center of the lesion, but only a hemorrhagic area with inflammatory cells and debris. In the fibrotic scar (Figure 8a & b), revascularization of the initial lesion began with growth of sinusoidal capillaries. Very few undamaged vessels were observed at the rim of the lesion only. In the first week, numerous capillaries and small-sized vessels were seen in the pia dura and gradually “infiltrated” the lesion. During the second week the initial lesion was highly vascularized. The number of blood vessels gradually declined in the 11<sup>th</sup> week (Figure 8c).

**Functional recovery:** The dorsal column in mice contains the long ascending sensory fiber tracts of the fasciculi cuneatus and gracilis, and the long descending corticospinal motor tract. The sensory fibers are located in the superficial portion of the dorsal column, whereas the corticospinal fibers in the ventral-most region of the dorsal column. Immediately after their recovery from anesthesia, mice were paraplegic. Forty-eight hours after SCT animals continued to show no motion of hind limbs. At the end of the first week, there was a slight positive reaction in all tested trials. As time passed over the following weeks, mice began to develop a gradual improvement in the motion of hind limb joints. An increase in the angle of movement of single or multiple joints was evident. On pain withdrawal test, an increasing improvement of motion reaction to pain was observed from the first week on to the 11<sup>th</sup> week, but the first reaction on toe spread test was observed during the 2<sup>nd</sup> week (Figure 9). On rope walk test, a continuing

progress in mice performance was observed until week 11. On wire mesh descent test, mice showed a constantly improving performance which was more obvious in weeks 3<sup>rd</sup> and 8<sup>th</sup>. On hindfoot bar grab test, scores remained low until the 8<sup>th</sup> week, but a significant progress was observed in the performance of mice which continued to improve until the 11<sup>th</sup> week. On ropewalk test, scores appeared to have a continuous upgrading up to week 11<sup>th</sup>. With regard to motorscore, remarkably higher scores were noticed from the 5<sup>th</sup> on to the 8<sup>th</sup> week post SCT. Then, a slight progress was continuously observed until the 11<sup>th</sup> week (Figure 9).

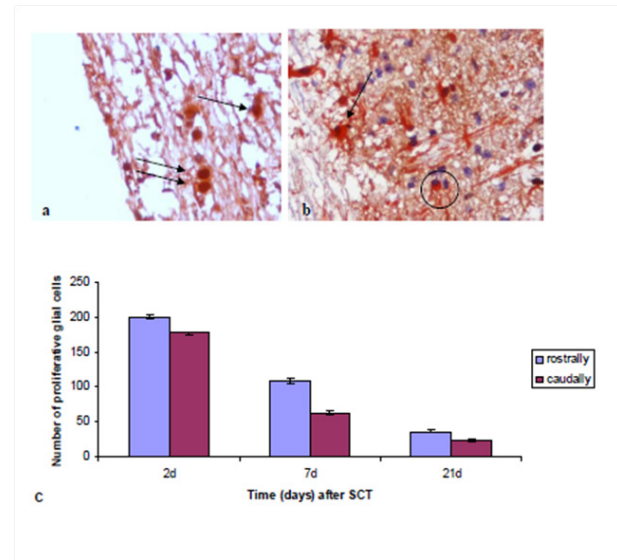


**Figure 7** Double stain for proliferative glial cells in white matter. a &b. Positive cells expressed red cytoplasm (S-100) and dark brown nucleus (Ki-67) (arrows). The enclosed cell, b. was a non-proliferative cells expressing only red chromogen in cytoplasm and hematoxylin nucleus. c. Proliferative glial cells appeared in large numbers two days after SCT trying to restore cellular loss and demyelination of neuronal axons. Their number declined dramatically after three weeks.

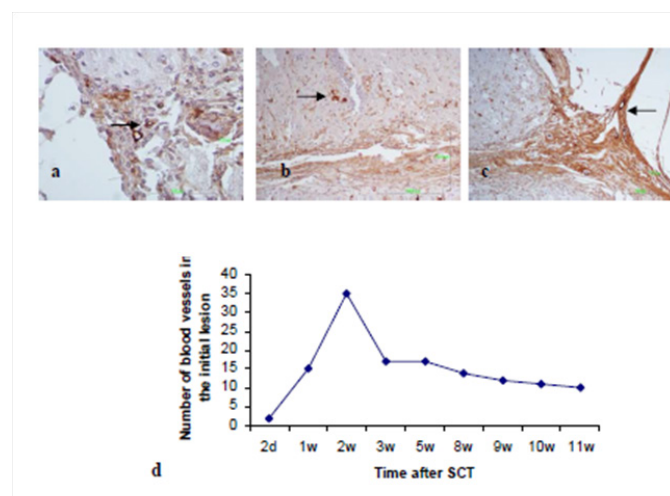


**Figure 8** a,b. Immunohistostain for the endothelial marker CD34. The initial lesion began to vascularize from the 1<sup>st</sup> week with numerous capillaries and small-sized vessels deriving the chorionic dura (a; arrow). Also well-formed vessels were seen around the central canal (b; arrow). c. The dura mater participated in the vascularization of the fibrotic scar (arrow). d. During the second week the initial lesion was highly vascularized and then the number of blood vessels declined significantly.

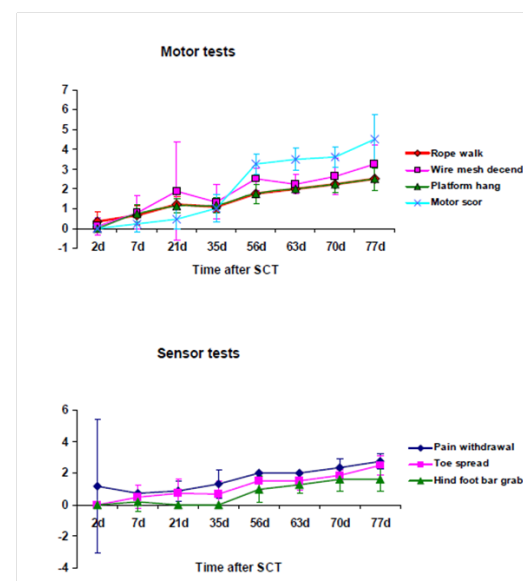


**Figure 9** Functional recovery was assessed by 4 motor and 3 sensor tests. On pain withdrawal test and toe spread test, an increasing improvement of motion reaction to pain was observed from the 1<sup>st</sup> and 2<sup>nd</sup> week on to the 11<sup>th</sup> week. On the rope walk test, mice performance appeared to progress constantly until week 11. On the wire mesh descent test, mice exhibited a constantly improving performance which was more obvious in weeks 3 and 8. On hind foot bar grab test, scores remained low until the 8<sup>th</sup> week but a significant increase was observed thereafter. On rope walk test, scores appeared to have an homogeneous upgrading up to week 11. The motor score were remarkably high from the 5<sup>th</sup> to the 8<sup>th</sup> week and a slight progress was continuously observed until week 11.

## Discussion

The goal of this study was to investigate the unique wound-healing response to severe spinal cord injury in C57bl/6 mice. Our findings demonstrated that a complete spinal cord transection in mice leads to a significant functional and histological recovery after the second week. Endogenous neurogenesis in the first three weeks involved proliferating glial and not neuronal cells. Glial cells seemed to be able to almost completely restore cellular loss, to remyelinate spared axons, and to support the rest undamaged neurons, resulting in functional recovery. The injured spinal cord area increased in size to a maximum during the first two weeks post SCT and then decreased steadily, until it was self-limited in the gray matter in the 11<sup>th</sup> week.

## Mouse model

The use of mice models for SCT, especially transgenic strains, has recently gained in practice compared to rat models. Almost all injury models performed in rats are equally reproducible in mice (crush and contusive injury, hemi-transection, transection, ischemic injury).<sup>3,5,9-12</sup> In the present study, we used a reproducible adult mouse spinal cord complete transection model, also cutting the dura mater, without laminectomy, accessing the cord through the inter vertebral spaces between two vertebral arches. This is a near-aggressive procedure in which the meanings are directly injured, causing disruption of cerebrospinal fluid dynamics and increasing connective tissue scarring. Surprisingly, despite the severity of spinal cord injury, animals showed almost complete functional and histological recovery after transection, without any therapeutic intervention. The first signs of functional recovery began already one week after the injury but the greater regain of motor function was observed after the 8<sup>th</sup> week. The

regain of early motor function could be explained by extra pyramidal system bridging, which can find the appropriate axonal targets.<sup>5</sup> The late motor regain was probably due to complete reconnection of neuronal axons of the white matter in lateral and posterior funiculus.

### Histological recovery

Mice undergo a different and unique histologic response to spinal cord injury from other mammals including rats and humans. In other species, SCT triggers secondary degenerative responses which lead to expansion of the lesion site, leaving behind fluid-filled cavities, a process that has been termed *progressive necrosis*. This is the result of ischemia, hypoxia, endothelial damage and degeneration of oxidative metabolism.<sup>3,13-16</sup> Functional recovery in these species is slow and limited. On the other hand, recent studies have shown that the mouse spinal cord is capable of functionally overcoming complete transactional injuries because, in general, the mouse does not show extensive secondary tissue loss.<sup>5,7,8,11,14</sup> These studies show that by overcoming the fibroblastic infiltrate and the displacement of the ends, and by leaving the dura essentially intact, functional regeneration can be induced without therapeutic intervention.<sup>5,17,19</sup> In our study, although the dura was cut, mice achieved satisfactory functional improvement. The lesion of the spinal cord was asymmetric as were the restoration and remyelination of the white and gray matter. The lesion length was greater in the white than in gray matter (Figure 10). The maximum average extent of the lesion was observed in the 2<sup>nd</sup> week, showing that the axotomized neurons initiate Wallerian degeneration of ascending fibers in a cranial direction and of descending fibers in a caudal direction. "Red neurons" located mainly in the cranial site of the lesion, appeared in the 1<sup>st</sup> week and increased in number until the 9<sup>th</sup> week. They remained after restoration indicating that neurons continue to undergo ischemic alterations. In the 5<sup>th</sup> week, the first signs of fibrotic scar auto-reversion appeared in the white matter, allowing the astrocytic network to penetrate into the connective tissue and reconnect the neuronal axons. Micro glial nodules composed of oligodendrocytes and macrophages also played a favorable role in recovery, as they penetrated into the fibers of the connective tissue, reducing cavitation and restoring remyelination. After the 5<sup>th</sup> week the restoration had an accelerated course despite the dramatic initial lesion and the cut dura. The role of the dura matter in restoration of the lesion is controversial because it contributes to scar formation but also provides vessels to the initial lesion. During the 2<sup>nd</sup> week the initial lesion was highly vascularized providing trophic and metabolic support essential for wound healing.

### Cell proliferation after spinal cord transection

In our study there are two important points with regard to restoration:

- glial cells proliferated in the dorsal column and in the gray matter around the initial lesion
- no neuron bodies were found among the dividing cells.

Forty eight hours after transection, proliferative glial cells constituted the cellular response to spinal cord damage, especially in the cranial site. Their number declined a week later and even more after three weeks. Dividing astrocytes showed peri neuronal "satellitosis" supporting the remaining neuron cells and creating reactive astrogliosis, which was a response to injury. They were found in great numbers at the rim of the initial lesion but they extended far beyond the borders of the damaged gray matter. Additionally, proliferative oligodendrocytes appeared in large numbers two days after SCT, trying to restore their cellular loss and probably to

remyelinate neuronal axons. Their number declined after three weeks, although scattered cells were found in micro glial nodules until five weeks after SCT. Their distribution in the white matter followed the expansion of the Wallerian degeneration, and the largest number of proliferative cells was found in the cranial site at the rim of the lesion. Proliferation of glial cells seemed to take place in the first hours after damage, although the injured site developed progressively until the 3<sup>rd</sup> week. They were not found in the initial lesion or inside the fibrotic scar. According to literature, glial cell proliferation is a direct response to SCT and part of the endogenous recovery mechanism that permits chronic glial repopulation of the injured spinal cord.<sup>20-24</sup> In addition, oligodendrocyte and astrocyte transplantations improve tissue sparing and functional recovery.<sup>25,26</sup> Recent studies have indicated that up-regulation of specific growth factors after contusive SCT is causally related to increased glial progenitor cell proliferation and chronic recovery of glial cell density.<sup>22,27</sup> Considerable evidence implicates scar-forming astrocytes as inhibitors of axon regeneration, and in this context, reactive astrocytes are widely regarded as detrimental to the overall outcome after SCT.<sup>28-32</sup> However, scar-forming, reactive astrocytes might exert a number of positive roles, i.e. repairing the blood-brain barrier, restricting leukocyte infiltration, protecting various neural elements, and preserving motor function.<sup>33,34</sup>

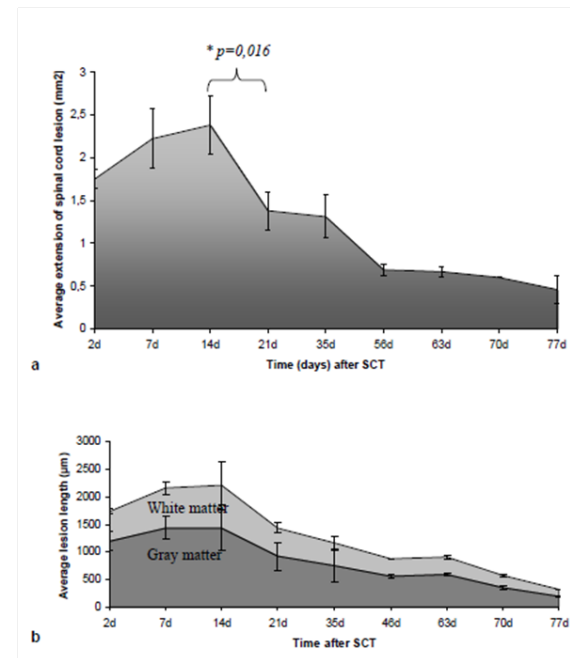


Figure 10

- The maximum extent of the white and gray matter lesion was observed in the 2<sup>nd</sup> week. Recovery began after the 2<sup>nd</sup> week and was statistically significant between 2<sup>nd</sup> and 3<sup>rd</sup> week.
- The average lesion length of white matter was greater than that of the gray matter.

The second major finding of our study is that SCT did not trigger the endogenous proliferation of neurons. Neither in a control, undamaged, mouse, nor in the transected animals was any neuronal body found positive for Ki-67 and synaptophysin markers. This finding is consistent with studies in rodents reporting extensive glial differentiation of newly born cells after contusive injury, and also with the contention that newly dividing cells in the intact spinal cord adopt glial and not neuronal fate.<sup>22,35-37</sup> In a recent study of hemi-transection injury in monkeys, 15% of proliferative new cells expressed mature

markers of oligodendrocytes and 12% expressed mature astrocytic markers by 7 months after injury, but no neuron formation was found. Newly born oligodendrocytes were present in zones of injury-induced demyelination and appeared to en sheath or remyelinate axons.<sup>38</sup> However, there is one report of neuronal differentiation in rodents after the administration of “stimulating agents”, such as neurogenin-2 or growth factors, i.e. fibroblastic growth factor 2 and epidermal growth factor.<sup>38</sup>

In short:

- A. Complete spinal cord transection including cut dura in C57bl/6 mice leads to almost complete functional recovery.
- B. The initial lesion, scar formation, and Wallerian degeneration of the white and gray matter regress drastically after the 5<sup>th</sup> week post injury.
- C. Immunophenotype analysis of the proliferative cells reveals that endogenous neurogenesis consists of the glial, and not of the neuronal cell-type proliferation.
- D. Intense proliferation of glial cells occurs in the first 48 hours after injury and declines thereafter. These findings underline the importance of early therapeutic intervention within the first hours after injury by using therapeutic agents that induce endogenous neurogenesis, which might stimulate not only the endogenous glial, but also the neuronal cell-type proliferation.

## Acknowledgments

None.

## Conflicts of interest

None.

## References

1. Tuszyński M, Edgerton R, Dobkin B. Recovery of locomotion after experimental spinal cord injury: axonal regeneration or modulation of intrinsic spinal cord walking circuitry? *J Spinal Cord Med Summer*. 1999;22(2):143.
2. Tuszyński MH, Gabriel K, Gerhardt K, et al. Human spinal cord retains substantial structural mass in chronic stages after injury. *J Neurotrauma*. 1999;16(6):523–531.
3. Zhang Z, Fujiki M, Guth L, Steward O. Genetic influences on cellular reactions to spinal cord injury: a wound-healing response present in normal mice is impaired in mice carrying a mutation (WldS) that causes delayed Wallerian degeneration. *J Comp Neurol*. 1996;371(3):485–495.
4. Fujiki M, Zhang Z, Guth L, et al. Genetic influences on cellular reactions to spinal cord injury: activation of macrophages/microglia and astrocytes is delayed in mice carrying a mutation (WldS) that causes delayed Wallerian degeneration. *J Comp Neurol*. 1996;371(3):469–484.
5. Seitz A, Aglow E, Heber Katz E. Recovery from spinal cord injury: a new transection model in the C57Bl/6 mouse. *J Neurosci Res*. 2002;67(3):337–345.
6. Inman DM, Steward O. Ascending sensory, but not other long-tract axons, regenerate into the connective tissue matrix that forms at the site of a spinal cord injury in mice. *J Comp Neurol*. 2003;462(4):431–449.
7. Joshi M, Fehlings MG. Development and characterization of a novel, graded model of clip compressive spinal cord injury in the mouse: Part I. Clip design, behavioral outcomes, and histopathology. *J Neurotrauma*. 2002;19(2):175–190.
8. Fernández López B, Romaus Sanjurjo D, Cornide Petronio ME, et al. Full anatomical recovery of the dopaminergic system after a complete spinal cord injury in lampreys. *Plast*. 2015;350750.
9. Seki T, Hida K, Tada M, et al. Graded contusion model of the mouse spinal cord using a pneumatic impact device. *Neurosurgery*. 2002;50(5):1075–1081.
10. Seki T, Hida K, Tada M, et al. Role of the bcl-2 gene after contusive spinal cord injury in mice. *Neurosurgery*. 2003;53(1):192–198.
11. Dong H, Fazzaro A, Xiang C, et al. Enhanced oligodendrocyte survival after spinal cord injury in Bax-deficient mice and mice with delayed Wallerian degeneration. *J Neurosci*. 2003;23(25):8682–8691.
12. Gaviria M, Hatton H, Sandillon F, et al. A mouse model of acute ischemic spinal cord injury. *J Neurotrauma*. 2002;19(2):205–221.
13. Hill RL, Zhang YP, Burke DA, et al. Shields CB. Anatomical and functional outcomes following a precise, graded, dorsal laceration spinal cord injury in C57BL/6 mice. *J Neurotrauma*. 2009;26(1):1–15.
14. Zhang Z, Guth L. Experimental spinal cord injury: Wallerian degeneration in the dorsal column is followed by revascularization, glial proliferation, and nerve regeneration. *Exp Neurol*. 1997;147(1):159–171.
15. Martinez M, Rossignol S. Changes in CNS structures after spinal cord lesions implications for BMI. *Prog Brain Res*. 2011;194:191–202.
16. Butenschön J, Zimmermann T, Schmarowski N, et al. PSA-NCAM positive neural progenitors stably expressing BDNF promote functional recovery in a mouse model of spinal cord injury. *Stem Cell Res Ther*. 2016;7(1):11.
17. Ma M, Basso DM, Walters P, et al. Behavioral and histological outcomes following graded spinal cord contusion injury in the C57Bl/6 mouse. *Exp Neurol*. 2001;169(2):239–254.
18. McTigue DM, Wei P, Stokes BT. Proliferation of NG2-positive cells and altered oligodendrocyte numbers in the contused rat spinal cord. *J Neurosci*. 2001;21(10):3392–4000.
19. McTigue DM, Popovich PG, Jakeman LB, et al. Strategies for spinal cord injury repair. *Prog Brain Res*. 2000;128:3–8.
20. Zai LJ, Yoo S, Wrathall JR. Increased growth factor expression and cell proliferation after contusive spinal cord injury. *Brain Res*. 2005;1052(2):147–155.
21. Zai LJ, Wrathall JR. Cell proliferation and replacement following contusive spinal cord injury. *Glia*. 2005;50(3):247–257.
22. Rosenberg LJ, Zai LJ, Wrathall JR. Chronic alterations in the cellular composition of spinal cord white matter following contusion injury. *Glia*. 2005;49(1):107–120.
23. Bambakidis NC, Miller RH. Transplantation of oligodendrocyte precursors and sonic hedgehog results in improved function and white matter sparing in the spinal cords of adult rats after contusion. *Spine J*. 2004;4(1):16–26.
24. Li N, Leung GK. Oligodendrocyte Precursor Cells in Spinal Cord Injury: A Review and Update. *Biomed Res Int*. 2015;235195.
25. Zhang C, Zhang G, Rong W, et al. Oscillating field stimulation promotes spinal cord remyelination by inducing differentiation of oligodendrocyte precursor cells after spinal cord injury. *Biomed Mater Eng*. 2014;24(6):3629–3636.
26. Bregman BS, Kunkel-Bagden E, Reier PJ, et al. Recovery of function after spinal cord injury: mechanisms underlying transplant-mediated recovery of function differ after spinal cord injury in newborn and adult rats. *Exp Neurol*. 1993;123(1):3–16.
27. Bush TG, Puvanachandra N, Horner CH, et al. Leukocyte infiltration, neuronal degeneration, and neurite outgrowth after ablation of scar-forming, reactive astrocytes in adult transgenic mice. *Neuron*. 1999;23(2):297–308.
28. Davies SJ, Goucher DR, Doller C, et al. Robust regeneration of adult sensory axons in degenerating white matter of the adult rat spinal cord. *J Neurosci*. 1999;19(14):5810–5822.

29. Menet V, Prieto M, Privat A, et al. Axonal plasticity and functional recovery after spinal cord injury in mice deficient in both glial fibrillary acidic protein and vimentin genes. *Proc Natl Acad Sci U S A*. 2003;100(15):8999–9004.
30. Levine J, Kwon E, Paez P, et al. Traumatically injured astrocytes release a proteomic signature modulated by STAT3-dependent cell survival. *Glia*. 2015;64(5):668–694.
31. Faulkner JR, Herrmann JE, Woo MJ, et al. Reactive astrocytes protect tissue and preserve function after spinal cord injury. *J Neurosci*. 2004;24(9):2143–2155.
32. Wu D, Shibuya S, Miyamoto O, et al. Increase of NG2-positive cells associated with radial glia following traumatic spinal cord injury in adult rats. *J Neurocytol*. 2005;34(6):459–469.
33. Alghamdi B, Fern R. Phenotype overlap in glial cell populations: astroglia, oligodendroglia and NG-2(+) cells. *Front Neuroanat*. 2015;9:49.
34. Horner PJ, Thallmair M, Gage FH. Defining the NG2-expressing cell of the adult CNS. *J Neurocytol*. 2002;31(6–7):469–480.
35. Lipson AC, Horner PJ. Potent possibilities: endogenous stem cells in the adult spinal cord. *Prog Brain Res*. 2002;137:283–297.
36. Yang H, Lu P, McKay HM, et al. Endogenous neurogenesis replaces oligodendrocytes and astrocytes after primate spinal cord injury. *J Neurosci*. 2006;26(8):2157–2166.
37. Xu L, Ryu J, Hiel H, et al. Transplantation of human oligodendrocyte progenitor cells in an animal model of diffuse traumatic axonal injury: survival and differentiation. *Stem Cell Res Ther*. 2015;6:93.
38. Ohori Y, Yamamoto S, Nagao M, et al. Growth factor treatment and genetic manipulation stimulate neurogenesis and oligodendrogenesis by endogenous neural progenitors in the injured adult spinal cord. *J Neurosci*. 2006;26(46):11948–11960.